Research Square

Preprints are preliminary reports that have not undergone peer review.
They should not be considered conclusive, used to inform clinical practice,
or referenced by the media as validated information.

Indoor microclimate shapes resting patterns of Anopheles funestus in south-eastern Tanzania

Polius G. Pinda

ppinda@ihi.or.tz

Ifakara Health Institute

Dickson S. Msaky
Ifakara Health Institute

Gustav Mkandawile
Ifakara Health Institute

Samwel Makayula
Ifakara Health Institute

Douglas E. Norris
Johns Hopkins Bloomberg School of Public Health

Michael R. Reddy
Microsoft Corporation, 1 Microsoft Way

Isaiah Hoyer
Microsoft Corporation, 1 Microsoft Way

Antoine Cribellier
Wageningen University & Research

Constantianus J.M. Koenraadt
Wageningen University & Research

Florian T. Muijres
Wageningen University & Research

Fredros O. Okumu
University of Glasgow

Emmanuel W. Kaindoa
Ifakara Health Institute

Research Article

Keywords: Indoor, Microclimate, Microhabitat, Anopheles funestus, Resting behaviour, House structure, House zones, and Vector control

Posted Date: September 1st, 2026

DOI: https://doi.org/10.21203/rs.3.rs-10776175/v1

License: This work is licensed under a Creative Commons Attribution 4.0 International License.
Read Full License

Additional Declarations: No competing interests reported.

Indoor microclimate shapes resting patterns of *Anopheles funestus* in south-eastern Tanzania

Polius G. Pinda[1,2,3*], Dickson S. Msaky[1,4], Gustav Mkandawile[1], Samwel Makayula[1], Douglas E. Norris[5], Michael R. Reddy[6], Isaiah Hoyer[6], Antoine Cribellier[3], Constantianus J.M. Koenraadt[7], Florian T. Muijres[3], Fredros O. Okumu[1,2,4,8], Emmanuel W. Kaindoa[1,2,4]

1. Environmental Health and Ecological Sciences Department, Ifakara Health Institute, Morogoro, United Republic of Tanzania.
2. Faculty of Health Sciences, School of Pathology, The Centre for Emerging Zoonotic and Parasitic Diseases, Wits Research Institute for Malaria, National Institute for Communicable Diseases, University of the Witwatersrand, Johannesburg, South Africa.
3. Experimental Zoology Group, Department of Animal Sciences, Wageningen University, Wageningen, The Netherlands.
4. School of Life Sciences and Biotechnology, Nelson Mandela African Institution of Science and Technology, Arusha, United Republic of Tanzania.
5. The W. Harry Feinstone Department of Molecular Microbiology and Immunology, The Johns Hopkins Malaria Research Institute, Johns Hopkins Bloomberg School of Public Health, Baltimore, USA.
6. Microsoft Premonition, Microsoft Corporation, 1 Microsoft Way, Redmond, USA
7. Laboratory of Entomology, Department of Plant Sciences, Wageningen University, Wageningen, The Netherlands.
8. Institute of Biodiversity, Animal Health and Comparative Medicine, University of Glasgow, Glasgow, UK.

*Corresponding author

Polius G. Pinda: ppinda@ihi.or.tz

E-mails

1. Polius G. Pinda: ppinda@ihi.or.tz (Orcid 0000-0002-9167-1672)

2. Dickson S. Msaky: dmsaky@ihi.or.tz
3. Gustav Mkandawile: gmkandawile@ihi.or.tz
4. Samwel Makayula: smakayula@ihi.or.tz
5. Douglas E. Norris: douglas.norris@jhu.edu (Orcid 0000-0002-4631-2777)
6. Michael R. Reddy: michael.reddy@microsoft.com (Orcid 0000-0001-8371-8306)
7. Isaiah Hoyer: Isaiah.Hoyer@microsoft.com
8. Antoine Cribellier: antoine.cribellier@wur.nl (Orcid 0000-0001-5113-7531)
9. Constantianus J.M. Koenraadt: sander.koenraadt@wur.nl
10. Florian T. Muijres: florian.muijres@wur.nl
11. Fredros O. Okumu: fredros@ihi.or.tz
12. Emmanuel W. Kaindoa: ekaindoa@ihi.or.tz

Abstract

Background: Indoor resting patterns of malaria vectors are changing, potentially driven by housing design including roofing materials, wall construction and associated indoor thermal and humidity-steered microclimates. This study quantifies how microclimatic gradients shape the resting choices of *Anopheles funestus* in southeastern Tanzania, testing whether different indoor zones create distinct thermal and humidity niches that influence mosquito microhabitat selection.

Methods: Between November 2024 and January 2026, thirteen sentinel houses, representing variation in house materials, roofing (metal or grass thatched), and wall material (bricks or mud) were sampled three times a week. In each house, mosquitoes were collected from indoor bottom, mid and top section using Prokopack aspirators. Sampling occurred in the morning (6:00-9:00h) or afternoon (12:00-15:00h). Indoor temperature and relative humidity were recorded at 30-minute intervals. Associations between house materials and zone, microclimate and resting behaviour were analysed using mixed-effect models.

Results: Across 153 sampling days, 1,910 *An. funestus* were collected. Most of these rested near the bottom house-section (40%), while the top-section had the smallest proportion (27%) ($p = 0.012$). Brick-walled houses had 80% higher abundance than mud-walled houses ($p < 0.001$), and grass-thatched houses had a 52% higher mosquito abundance than metal-roofed houses ($p = 0.002$). Indoor thermal microhabitats matched mosquito resting patterns, as both temperature and humidity varied between house materials and zones. The strong negative correlation between temperature and relative humidity ($r = -0.738$) limited the explanatory value of relative humidity, whereas the weaker correlation between temperature and absolute humidity enabled separation of temperature and humidity effects on resting behaviour. Abundance of resting *An. funestus* was associated with the joint interaction of mean temperature ($\bar{T}$), temperature fluctuations (T_{range}), and absolute humidity ($\overline{\text{AH}}$), with highest abundance near $\bar{T}$=32.7°C and $\overline{\text{AH}}$=16.4 g/m³, and for minimal temperature fluctuations (T_{range}≈0°C).

Conclusion: The joint interaction between mosquito abundance, resting stratification and environmental variables (temperature and humidity) explains indoor resting patterns of *An. funestus*. These highlight the importance of incorporating indoor microclimatic heterogeneity

into vector control strategies where housing improvements could alter indoor suitability for mosquito resting, survival, and malaria transmission.

Keywords: Indoor, Microclimate, Microhabitat, *Anopheles funestus*, Resting behaviour, House structure, House zones, and Vector control.

Background

The global malaria burden is disproportionally concentrated in sub-Saharan Africa, accounting for over 90%, particularly among children under five [1,2]. Although substantial progress has been achieved in the early 2000s in reducing malaria incidence and deaths, gains have plateaued since 2015, with a slight resurgence observed in 2020 [1]. These setbacks have been attributed to increasing insecticide resistance, funding constraints, the SARS corona virus disease 2019 (COVID-19) pandemic, changing climate and extreme weather conditions, and shifts in mosquito behaviours [1,3]. Nevertheless, integrated vector and parasite control strategies remain indispensable to achieving the elimination goal [4].

Insecticide treated nets (ITNs) and indoor residual spraying (IRS) are the most commonly used vector control tools [4,5], providing physical and insecticidal protection against mosquito bites [5,6]. Although IRS is among the most effective vector control tools [7], its use has declined in numerous endemic countries due to its higher operational costs [8,9]. This challenge is further compounded by emerging behavioural shift among malaria vectors, increasingly resting on surfaces not targeted by IRS such as the floors and ceilings, and other household items, thereby reducing overall effectiveness [10]. Observed shifts might be attributed to species-specific resting ecology, insecticide avoidance or adaptive responses to indoor microclimatic variation driven by house structural features such as roofing and wall materials [11,12]. Studies have suggested partial and targeted indoor residual spraying to counteract the observed resting behavioural shift of major malaria vectors, thereby improving intervention effectiveness while reducing operational costs [10,13–17].

Evidence from multiple African settings indicates that major malaria vectors, including *Anopheles arabiensis*, *An. funestus*, *An. gambiae*, and *An. coluzzii* exhibit diverse indoor resting behaviours. For instance, findings in Ghana and Zimbabwe revealed that over 45% of the latter three species were either resting under the roof or other surfaces but fewer (≤ 40%) on the wall [14,18,19]. In contrast, *An. coluzzii* from Côte d'Ivoire exhibited predominant wall-resting behaviour (63%) compared to under-roof and other surfaces [13]. In southeastern Tanzania, a substantial proportion of *An. arabiensis* and *An. funestus* have been reported resting under roofs, with a clear preference for grass-thatched houses compared to iron-roofed houses [20].

Behavioural shifts in malaria vectors are becoming increasingly important as indoor environments are becoming progressively heterogeneous as a result of housing

transformation and urbanization. In many malaria-endemic regions, traditional houses are being replaced or modified with metal-sheet roofs, brick or cement walls, and altered ventilation systems, all of which substantially influence indoor temperature, humidity, and airflow dynamics [21–23]. These structural changes may alter indoor microclimates by altering heat retention, moisture regulation, and air circulation. For instance, metal-sheet roofs often enhance daytime heat accumulation, whereas grass-thatched roofs provide more thermally buffered and stable conditions [24]. Collectively, these variations generate distinct indoor microhabitats that may influence mosquito resting site selection and survival. These microhabitats are likely to be vertically stratified, extending from the house floor to the roof space, with each house zone characterized by unique microclimatic conditions. Moreover, these gradients vary throughout the day, with upper house zones becoming progressively warmer and drier during the day, while lower zones, including floors and lower wall surfaces, remain relatively cooler and more humid. However, whether observed mosquito behavioural shifts reflect species-specific resting ecology, microclimatic preferences, house structure, insecticide avoidance, or a synergistic interaction among these factors remains unclear.

Although several studies have highlighted the influence of house construction materials, far fewer have explicitly examined the role of housing-induced microclimate in shaping mosquito biting and resting patterns. Environmental temperature and humidity can either enhance or constrain mosquito development, survival, reproduction, and disease transmission depending on species-specific physiological thresholds [25,26]. Exposure to high but non-lethal temperatures accelerates mosquito development, potentially increasing population size and disease transmission. However, these benefits often occur at the cost of reduced adult survival, smaller body size, lower fecundity, and shortened gonotrophic cycles [27–31]. Ngowo *et al*. demonstrated that a 1°C increase of indoor temperature prompted *An. arabiensis* but not *An. funestus* to shift towards outdoor biting behaviour [32]. Such responses likely reflect species-specific thermal limits and tolerance ranges of both malaria vectors and the pathogens they carry, which may vary across developmental stages, physiological status, and genetic background [33–36]. Thus, behavioural adaptations such as selecting cooler and humid indoor microhabitats for resting during warmer periods might play a critical role in buffering mosquitoes against thermal stress.

This study aimed to investigate how indoor resting patterns of *An. funestus* are shaped by both housing characteristics and microclimatic conditions (temperature and humidity) in

south-eastern Tanzania. First, we quantified how house structure, including roof materials, wall material, and house zones (bottom, mid, top), influence mosquito resting behaviour. Second, we assessed how these structural features generate distinct indoor microclimates. Third, we quantified how mosquitoes respond to these environmental conditions, with the aim of identifying the temperature and humidity ranges that shape resting abundance. For the purposes of this study, microclimate refers to the temperature and humidity conditions measured directly on indoor surfaces (walls, floors, and under-roof spaces).

Methods

Study area

The study was conducted in two villages located approximately 50km apart in south-eastern Tanzania (**Fig. 1A**). The area comprises low-lying valley plains at approximately 150m above sea level, which rise sharply toward the neighbouring Udzungwa and Mahenge mountain ranges, exceeding 1,000 m in elevation. Local livelihoods are primarily based on rice cultivation and livestock keeping, and the area receives annual rainfall of approximately 1000 mm [37]. Malaria vector population is dominated by *An. arabiensis* and *An. funestus*, with the latter responsible for over 80% of malaria transmission even when being collected at lower densities than the former [38,39]. ITNs remain the primary vector control intervention in the area, with no history of IRS, while local vector populations exhibit resistance to commonly used insecticides [40,41].

House characterization and environmental conditions

Sampling houses were purposively selected to represent the most common construction materials in the study area. These included: (i) mud walls with a grass-thatched roof, (ii) mud walls with an iron roof, (iii) un-plastered brick walls with a grass-thatched roof, (iv) un-plastered brick walls with an iron roof (**Fig. 1B**). Indoor house surfaces were categorized into three mosquito sampling zones, the bottom, middle, and top sections of the house, hereafter referred to as microhabitats. This classification incorporated both bare surfaces and associated structural components. For instance, the bottom section comprised the bare floor, objects located within approximately 30 cm above the ground (e.g. furniture and utensils), and the lower 30 cm of the wall (**Fig. 1C**). The top section included the upper 30 cm of the wall and under-roof surfaces while the midsection included wall surfaces above the bottom section and below the top section. Data loggers (HOBO MX1101 Temp/RH; accuracy ±0.21 °C and ±2% RH) were installed on each predefined mosquito sampling surface,

precisely on the floor, mid-wall, and directly under the roof, continuously recording temperature and relative humidity (**Fig. 1C**). To capture both diurnal and seasonal fluctuations, loggers were configured at 30-minute data capturing intervals throughout the study period.

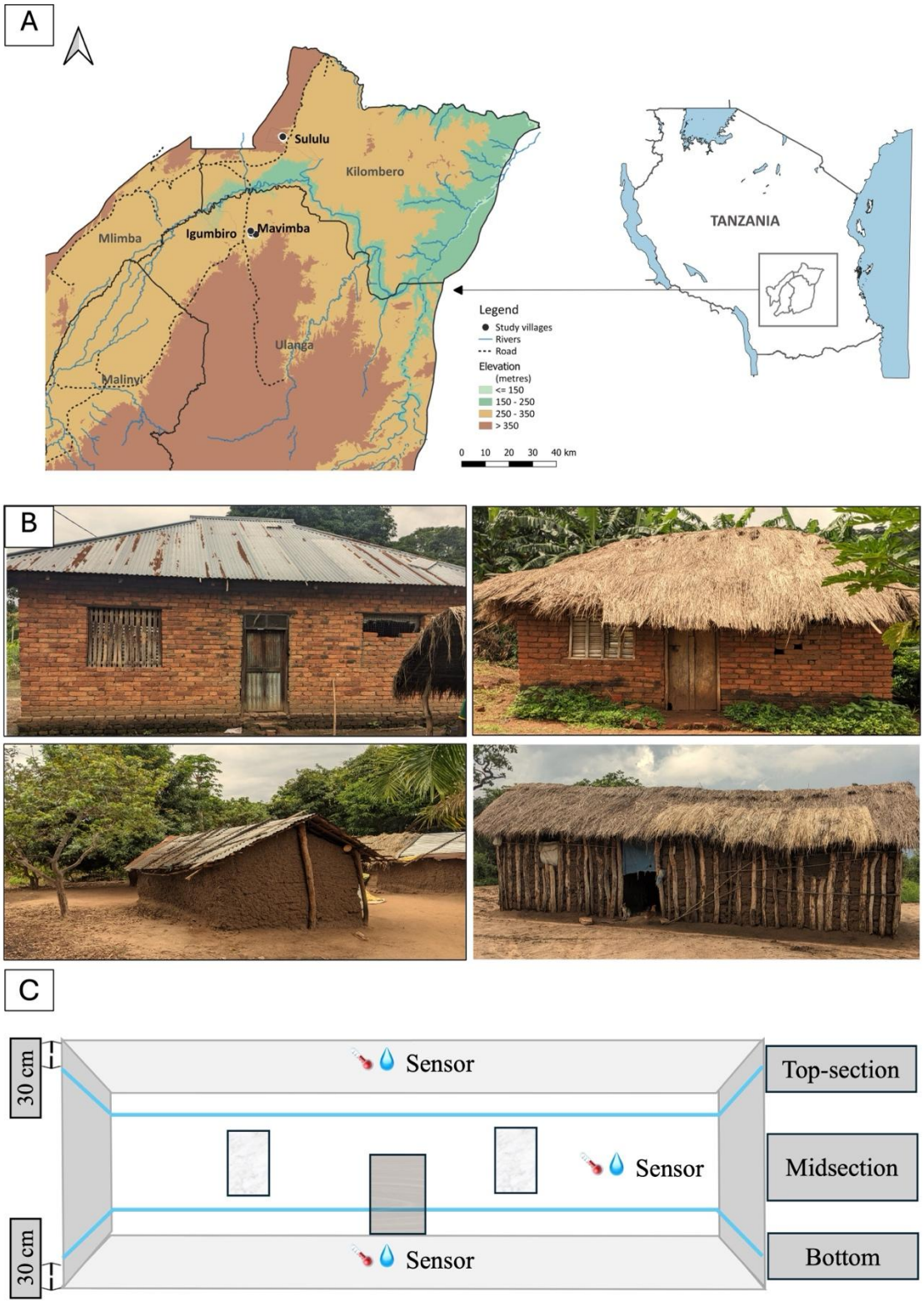


Figure 1. Map of the study area showing the study village locations in south-eastern Tanzania (A) Six and seven houses were sampled in Igumbiro and Sululu villages respectively. (B) Sampled houses examples by construction materials, separated into roof materials on the horizontal (metal or grass thatched) and wall materials on the vertical (mud or brick). (C) Indoor house schematic with classification of the resting surfaces (top, middle and bottom section), and section-specific environmental condition monitoring (temperature, humidity) using a climate data logger (HOBO MX1101).

Mosquito sampling strategy

Indoor resting mosquito collections were conducted using Prokopack aspirators [42] (John W. Hock Company, Florida, USA) between November 2024 and January 2026 with a total of 153 sampling days per house materials and surface. Aspiration procedures were done at least 30 cm away from the adjacent sampling surface to minimize disturbance and collecting mosquitoes from untargeted surface. A minimum of twelve collections per month (3 times per week) were undertaken in houses and maintained as sentinel to capture temporal variation in resting behaviour. To correlate mosquito resting microhabitats with daily fluctuations on indoor temperature and humidity, sampling was performed at two time points: morning (06:00 - 09:00) or midday (12:00 - 15:00). Each house was sampled once per day, either in the morning or midday, to represent diurnal resting patterns across the study period.

To minimize bias arising from mosquito movement during sampling, the order in which resting surfaces were aspirated (bottom, mid and top section of the house) was rotated daily. For instance, when sampling began on the walls on a given day, it would begin on the bottom or top section the following day. Collected mosquitoes were kept separately by surface on which they were collected and thereafter transported to Ifakara Health Institute laboratory for further processing. In this study, the “bottom section” category included the ground surface and any objects or items located within approximately 30 cm above the ground. The “top section” category includes top 30 cm of the wall and under-roof surface, predominantly with no ceiling.

Sample processing and identification

All *An. funestus* group mosquitoes were identified morphologically using the Gillies and Coetzee identification key [43,44]. Further laboratory analyses were conducted on a 20% subsample to identify sibling species, detect malaria parasites and identify blood meal

sources in blood-fed females. Sibling species within the *An. funestus* group were identified molecularly using polymerase chain reaction (PCR) assays targeting the non-coding internal transcribed spacer 2 (ITS2) region for *An. funestus* [45]. Enzyme linked immunosorbent (ELISA) assays were used to detect the presence of *Plasmodium falciparum* parasite-circumsporozoite proteins (CSP) in the salivary glands of *An. funestus* [46]. False positive results were eliminated by boiling ELISA lysate for 10 minutes at 100˚C, to effectively eliminate heat-labile non-*P. falciparum* parasite antigens and the samples were re-assayed [47]. Engorged mosquitoes were analysed for host bloodmeal identity by the antibody-sandwich ELISA to detect human, bovine, dog, goat, and chicken IgG [48]. Positive controls prepared from host sera and negative controls (laboratory reared, non-fed female mosquitoes prepared in the same way as the test samples) were included for each ELISA plate.

Microclimate sampling and variable definition

Indoor temperature (*T)* and relative humidity (RH) were continuously recorded at each pre-defined house microhabitat (bottom, mid, and top sections) using HOBO MX1101 Temp/RH data loggers (accuracy *T*: ±0.21 °C; accuracy RH: ±2%). Loggers were positioned directly on representative resting surfaces, including the bottom, mid, and top wall sections (**Fig 1C**), and recorded data at 30-minute intervals throughout the study period. To match environmental conditions with mosquito sampling, data were subsampled to the defined sampling windows (morning: 06:00-09:00; midday: 12:00-15:00). From temperature (*T*) and relative humidity (RH) we derived absolute humidity (AH) as water vapor content, in grams of H_2O per cubic meter air (g/m^{-3}) as

$$\mathrm{AH} = \frac{6.112 \cdot e^{\left(\frac{17.67\,T}{T+243.5}\right)} \cdot \mathrm{RH} \cdot 2.1674}{T+273.15}. \quad (1)$$

Environmental conditions were summarized for specific mean values and ranges per house, microhabitat, and sampling period. Metrics included mean temperature, relative humidity, and absolute humidity ($\overline{T}$, $\overline{\mathrm{RH}}$ and $\overline{\mathrm{AH}}$, respectively), as well as their corresponding ranges (T_{range}, $\mathrm{RH}_{\mathrm{range}}$ and $\mathrm{AH}_{\mathrm{range}}$, respectively). Means and ranges were calculated as the average and the central 95% of observed values within each sampling period, respectively.

Data analysis

All analyses were conducted in R version 4.5.0 [49]. The dataset was filtered to include only *An. funestus* mosquitoes. First, we quantified how house structure determines mosquito resting abundance. Second, we assessed how house structure generates variation in indoor microclimatic conditions, specifically temperature and humidity. Third, we evaluated how mosquito resting behaviour responds to these environmental conditions. This stepwise approach allows separation of structural effects from the underlying environmental mechanisms that drive mosquito resting site selection.

Analysis of mosquito resting abundance in different micro-habitats

In the first step, we quantified how house structure determines mosquito resting abundance across indoor microhabitats. The relationship between mosquito abundance and household characteristics (house zones, wall and roof materials), as well as sampling time, was evaluated using generalized additive models (GAMs) with a negative binomial distribution to account for overdispersion. Specifically, mosquito counts were modelled as

$$\log(N_p) = \text{House zone} + \text{Roof material} + \text{Wall material} + \text{Collection time} + s(\text{Date}) + (1 \mid \text{Day}),$$

where $s(\text{Date})$ represents a smooth function (cubic regression spline) of sampling date to capture seasonal variation.

Sampling day was included as a random effect to account for repeated measures, and interaction terms were included to capture potential context-dependent effects. Estimated marginal means (EMMs) and pairwise contrasts were calculated using the *emmeans* package [50] with Tukey adjustment.

Analysis of thermal and humidity conditions in different microhabitats

In the second step, we assessed how house structure generates variation in indoor microclimatic conditions across different in-house microhabitats. Environmental data were first quality-checked by excluding extreme outliers in temperature and relative humidity measurements before analysis. Daily mean temperature, temperature range, mean relative humidity, and relative humidity range were calculated for each house zone (bottom, midsection, and top section), roof materials, and wall material. Absolute humidity (g/m^3) was

subsequently derived from temperature and relative humidity values using the saturation vapour pressure equation (Eqn 1).

Mean daily environmental conditions (temperature and humidity means and ranges) were examined using generalized additive models (GAMs) with Gaussian errors, incorporating roof material, wall material, house zone, daytime, and household identity as fixed effects, including relevant interactions. Sampling round was included as a random effect to account for repeated observations. The models were specified with the environmental variable of interest (temperature or humidity metric) as the response variable and date as a smooth predictor term using cubic regression splines.

Analysis of effect of microclimate conditions on mosquito resting abundance

In the third step, we analysed how mosquito resting behaviour responds to indoor microclimatic conditions. We explored the joint distribution of mosquito abundance and environmental variables to assess how mosquito abundance co-varies with temperature and humidity across the observed environmental gradient. This step allowed us to evaluate the structure of the environmental space, identify potential dependencies among variables, and determine the extent to which temperature and humidity can be treated as independent predictors in subsequent modelling. We considered both relative humidity (RH) and absolute humidity (AH) to assess how temperature co-varies with different measures of atmospheric moisture and to guide variable selection for the subsequent analysis.

Third, we quantified these relationships using generalized linear models (GLMs) with a log link function, in which mosquito abundance was modelled as a function of mean temperature, mean humidity, and their corresponding ranges. Specifically, we defined the model as:

$$\log(N_p) = \beta_0 + \beta_1\overline{T} + \beta_2\overline{T}^2 + \beta_3\overline{H} + \beta_4\overline{H}^2 + \beta_5 T_{\text{range}} + \beta_6 H_{\text{range}},$$

where the humidity term H represents either absolute humidity (AH) or relative humidity (RH), which capture different aspects of atmospheric moisture. We therefore fitted models using both variables to assess their explanatory power.

We included quadratic terms for mean temperature and mean humidity to allow for unimodal physiological responses, while we included range variables as linear terms to represent the

effect of environmental variability. We evaluated model fits using Poisson and negative binomial error distributions to account for overdispersion, and final model selection followed standard criteria (model selection and statistical inference).

By acknowledging a non-linearity between mosquitoes and environmental conditions, optimal mean temperature ($\bar{T}_{\mathrm{opt}}$) and humidity ($\bar{H}_{\mathrm{opt}}$) values were computed from the model estimates as

$$\bar{T}_{\mathrm{opt}} = -\frac{\beta_1}{2\beta_2}, \qquad \bar{H}_{\mathrm{opt}} = -\frac{\beta_3}{2\beta_4}. \tag{2}$$

where β_1 and β_2 represent the linear and quadratic effects of temperature, respectively, while β_3 and β_4 represent the linear and quadratic effects of humidity, respectively. We did not include housing variables (house zone, roof material, wall material, and sampling time) in these models because they act by generating variation in temperature and humidity. Including these variables would reduce the environmental gradient and obscure the functional relationship between microclimate and mosquito behaviour.

To evaluate the joint effects of environmental variables, we constructed two-dimensional response surfaces from model predictions for combinations of temperature and humidity (mean and range). We further characterized the role of individual variables by deriving predicted abundance profiles from the fitted models while holding all other variables constant at their mean values.

Model selection and statistical inference

Model selection was guided by ecological relevance, biological interpretability, and information criteria (Akaike's Information Criterion, AIC, and Bayesian Information Criterion, BIC), ensuring that retained models captured the expected mechanistic relationships while avoiding overfitting. Overdispersion in count data was assessed by comparing Poisson and negative binomial model fits, with negative binomial models used where appropriate. Model assumptions were evaluated using residual diagnostics.

Effect sizes were quantified as standardized differences in model-predicted values divided by the residual standard deviation of the fitted model as

$$d = \frac{\Delta \text{ predicted values}}{\sigma_{residual}}. \quad (3)$$

This metric is equivalent to Cohen's *d* and reflects the magnitude of differences between conditions independently of sample size.

Differences were considered statistically significant when $p < 0.05$, and were interpreted as having a large effect size when $d \geq 0.5$ and a small effect size when $d < 0.5$. Differences that satisfied both criteria ($p < 0.05$ and $d \geq 0.5$) were considered both statistically significant and biologically meaningful. This combined interpretation allows distinguishing between statistically detectable differences and those that are also of ecological relevance. Where relevant, pairwise comparisons were performed using Wilcoxon tests with Bonferroni correction. All visualizations were generated using *ggplot2*.

Results

Indoor resting patterns of *Anopheles funestus*

A total of 1,910 indoor-resting *An. funestus* were collected across 153 sampling days (rounds). The majority of these mosquitoes was resting on the bottom section (40%, *n* = 758 mosquitoes), followed by the wall-midsection (33%, *n* = 640), and the smallest proportion recorded on the top section (27%, *n* = 512) (**Table 1**). With respect to house characteristics, *An. funestus* were collected more frequently from brick-walled houses (80%, *n* = 1,531) than from mud-walled houses (20%, *n* = 379). Similarly, grass-thatched roofs harboured a higher number of mosquitoes (52%, *n* = 993) than metal-roofed houses (48%, *n* = 917) (**Table 1**). To determine whether indoor microhabitats (bottom, mid, top sections), housing characteristics, and sampling time significantly influenced resting abundance, descriptive patterns were further evaluated using generalized additive models.

Table 1. Observed and generalized additive model predicted indoor-resting *An. funestus* distribution by collection timing, house zones, and house characteristics (roof and wall materials), excluding environmental parameters.

Predictors	**Categories**	**Sampled data**		**Predicted number**	
		Total (*n*)	**Proportion (*P*)**	**Mean ($\hat{\mu}$)**	**95% CI**
Collection time	06:00-09:00h	944	0.494	0.548	0.455 - 0.658

	12:00-15:00h	966	0.506	0.563	0.469 - 0.676
Roof materials	Grass-thatch	993	0.520	0.627	0.523 - 0.750
	Metal	917	0.480	0.492	0.410 - 0.591
House zone	Top section	512	0.268	0.469	0.383 - 0.573
	Midsection	640	0.335	0.554	0.455 - 0.675
	Bottom section	758	0.397	0.659	0.543 - 0.801
Wall materials	Bricks	1,531	0.802	1.128	0.952 - 1.338
	Mud	379	0.198	0.273	0.225 - 0.333

The estimated number of mosquitoes was significantly lower on the house top section compared to the bottom section ($\hat{\mu}$ =0.469 [0.383-0.573] and $\hat{\mu}$ =0.659 [0.543-0.801], respectively; mean [95% confidence interval]; p=0.012; **Fig. 2**). However, there was no significant difference between the bottom section and the wall-midsection (p=0.153). Importantly, mosquito abundance correlated with house structural characteristics, with metal roofs and mud-walled houses harbouring significantly lower mosquito numbers compared to grass-thatched and brick-walled houses (p<0.05; **Fig. 2**). Estimated means of indoor-resting *An. funestus* were not significantly different between the morning and afternoon sampling periods ($\hat{\mu}$ =0.548 [0.455-0.658] and $\hat{\mu}$ =0.563 [0.469-0.676]), respectively; p = 0.729; **Table 1, Fig. 2**).



Figure 2. Number of *An. funestus* mosquitoes collected by variable (collection time, roof material, house zone, and wall material), estimated using a generalized additive model, smoothing on sampling date. Each panel shows estimated marginal means and confidence intervals (emms±CI) per variable, while keeping all other variables at their mean value. Statistical significance between conditions is highlighted based on *p*-value as: *** (p<0.001); ** (p<0.01); * (p<0.05); "ns" (p>0.05).

Indoor microclimatic conditions

Thermal conditions within different indoor microhabitats

Indoor microhabitats (bottom, mid, and top house section) showed clear and consistent daily differences in thermal conditions. The bottom zone remained the coolest microhabitat, while the top zone was consistently the warmest, with mean temperatures of approximately 28°C and 31°C, respectively ($\Delta\bar{T}$ = 3.3°C, Cohen's d = 0.9, p<0.001; **Fig. 3C**). Similarly, the bottom section exhibited the lowest temperature fluctuation compared to the top section of the house (ΔT_{range} = 2.8°C, d = 1.2, p<0.001; **Fig. 4C)**. In contrast, the difference in mean temperature between the wall-midsection and the top zone was smaller but statistically significant ($\Delta\bar{T}$= 1.6°C, d = 0.45, p<0.001; **Fig. 3C**). Despite relatively small difference in

mean temperature, the wall-midsection and the top zone differed substantially in their diurnal temperature variability, with greater fluctuations observed in the top zone (ΔT_{range} = 2.0°C, d = 0.82, p<0.001; **Fig. 4C**).

Thermal conditions also varied markedly across sampling periods and house characteristics whereas mean indoor temperature was significantly higher during the midday sampling period (12:00–15:00 hrs) compared to the morning period (06:00 - 09:00 hrs) ($\Delta\bar{T}$= 5.6°C, d = 1.55, $p < 0.001$; **Fig. 3A**). The corresponding difference in temperature fluctuation between these periods was relatively small but statistically significant (ΔT_{range} = 0.5°C, d = 0.23, $p <$ 0.001; **Fig. 4A**). House structural characteristics further influenced indoor thermal environments where metal-roofed houses exhibited significantly higher mean temperatures ($\Delta\bar{T}$= 3.1°C, d = 0.86, $p < 0.001$) and greater temperature fluctuations (ΔT_{range} = 1.3°C, d = 0.56, $p < 0.001$) compared to grass-thatched houses **(Fig. 3B & 4B)**. In contrast, mud-walled houses tended to be cooler than brick-walled houses, although the effect sizes for both mean temperature and fluctuation were small ($d < 0.5$; **Fig. 3D & 4D**).

Humidity conditions among the different indoor microhabitats

Predictor categories with relatively higher temperatures consistently exhibited lower relative humidity than their respective counterparts (**Fig. 3E - H)**. Indoor microhabitats (bottom, mid, and top house section) showed a clear and consistent daily differences in humidity conditions (**Fig. 3G**). Except for wall materials which showed only statistical significance but smaller effect size, timing of the day, roof materials and indoor house zones had higher effect size and were statistically significant ($d > 0.5$, $p < 0.001$; **Fig. 3F-H**). Overall, the bottom section of the house was the least fluctuating and most humid zone compared to top section ($\Delta\overline{RH}$ = 6.5%, d = 0.5, $p < 0.001$). Additionally, metal roofed houses experienced drier and more variable humidity compared to grass-thatched houses ($\Delta\overline{RH}$ = 7.8%, d = 0.6, $p < 0.00$).

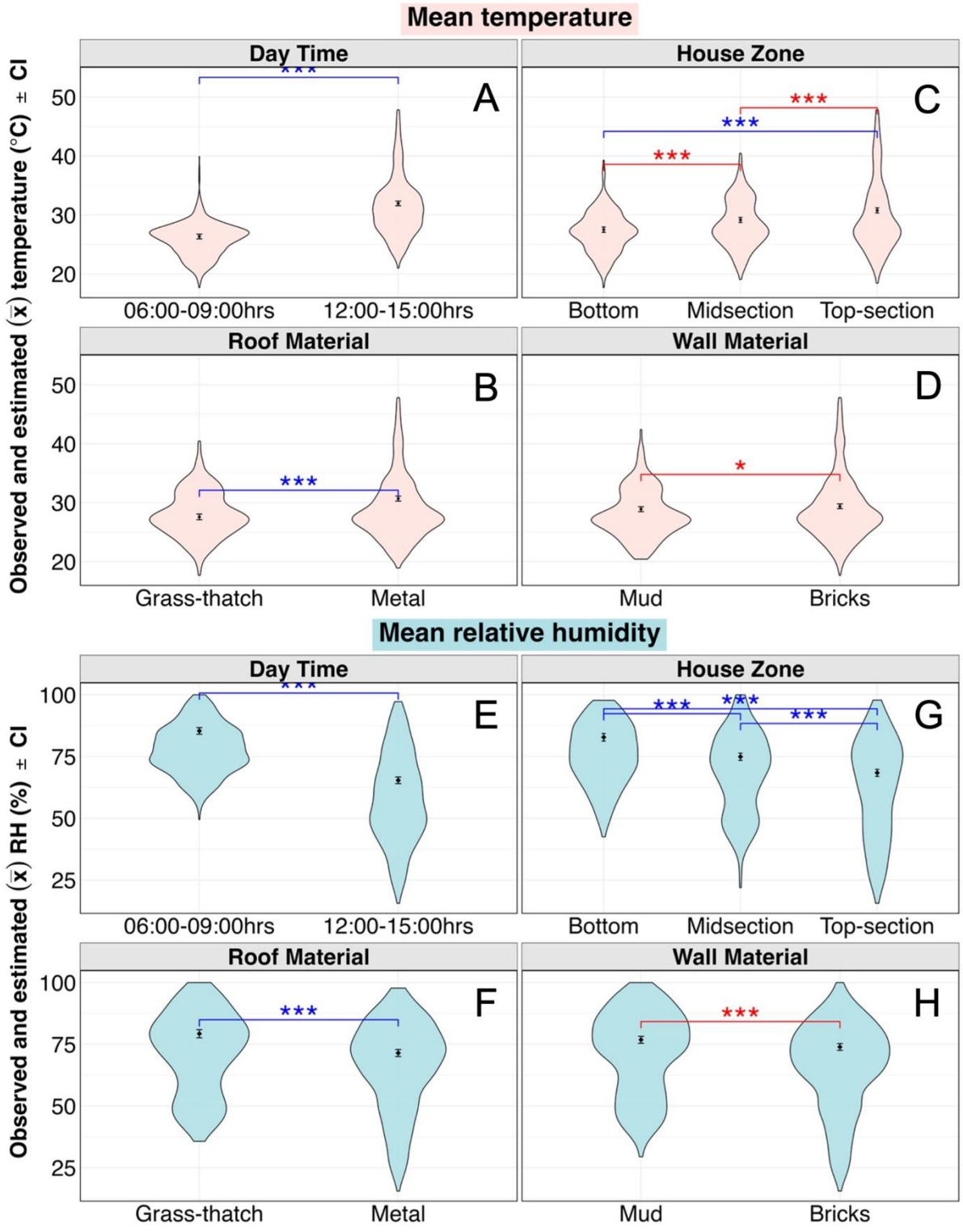


Figure 3. Indoor temperature and relative humidity mean across sampling periods, house zones, and structural house features (roof and wall materials). Violin plots show mean distributions for temperature (pale red; A - D) and relative humidity (pale blue; E - H). Data point with whiskers shows estimated means and their 95% confidence intervals. Coloured

square brackets with asterisks highlight significance (***: $p < 0.001$; **: $p < 0.01$; *: $p < 0.05$) and effect size (blue: $d \geq 0.5$; red: $d < 0.5$) between conditions.

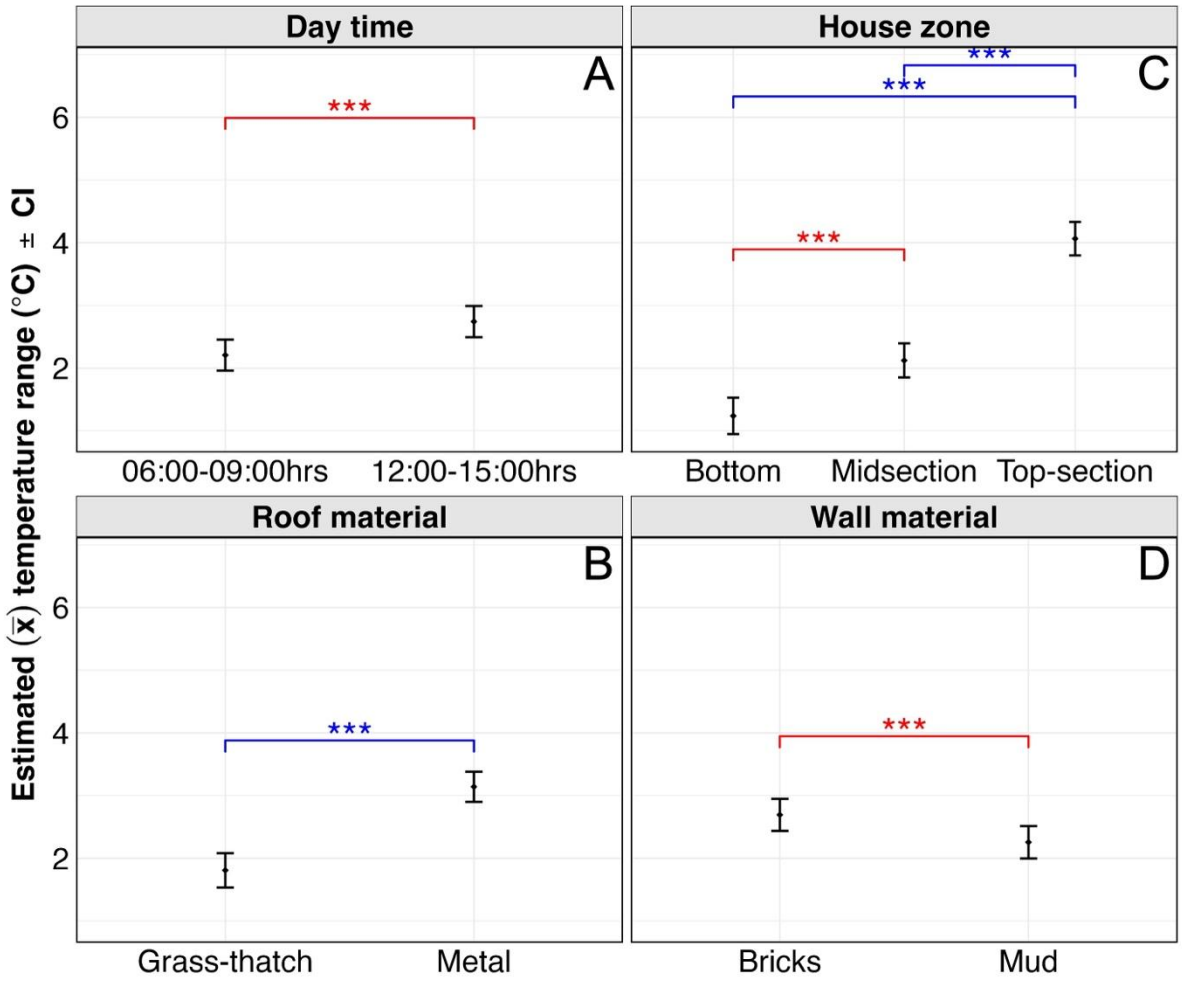


Figure 4. Indoor temperature range across sampling periods, house zones, and structural features (roof materials and wall materials). Data point with whiskers shows the estimated temperature range (mean ± 95% confidence interval). Coloured square brackets with asterisks highlight significance (***: $p < 0.001$) and effect size (blue: $d \geq 0.5$; red: $d < 0.5$) between conditions.

Interaction between temperature, humidity and *An. funestus* resting patterns

Diurnal abundance of *An. funestus* was highest within relatively narrow climatic limits characterized by mean temperatures of 25 - 35°C, absolute humidity levels of 15 - 25 g/m³, and diurnal temperature fluctuations below 5°C (**Fig. 5A - D**). High mosquito counts occurred across a wide range of relative humidity values, consistent with the strong negative correlation between temperature and relative humidity (r = -0.738), suggesting limited

explanatory value of relative humidity alone (**Fig. 5A**). In contrast, high counts clustered around the 15 - 25 g/m³ absolute humidity isolines, and the weak correlation between temperature and absolute humidity (r = 0.072) indicated that this relationship was largely independent of temperature (**Fig. 5B**). Elevated mosquito abundance was also restricted to environments with low diurnal temperature variability, with temperature ranges exceeding 5°C consistently associated with lower abundance (**Fig. 5C - D**). Consequently, absolute humidity was selected over relative humidity for subsequent modelling analyses due to limited explanatory power of relative humidity alone (**Supplementary Table S1**).

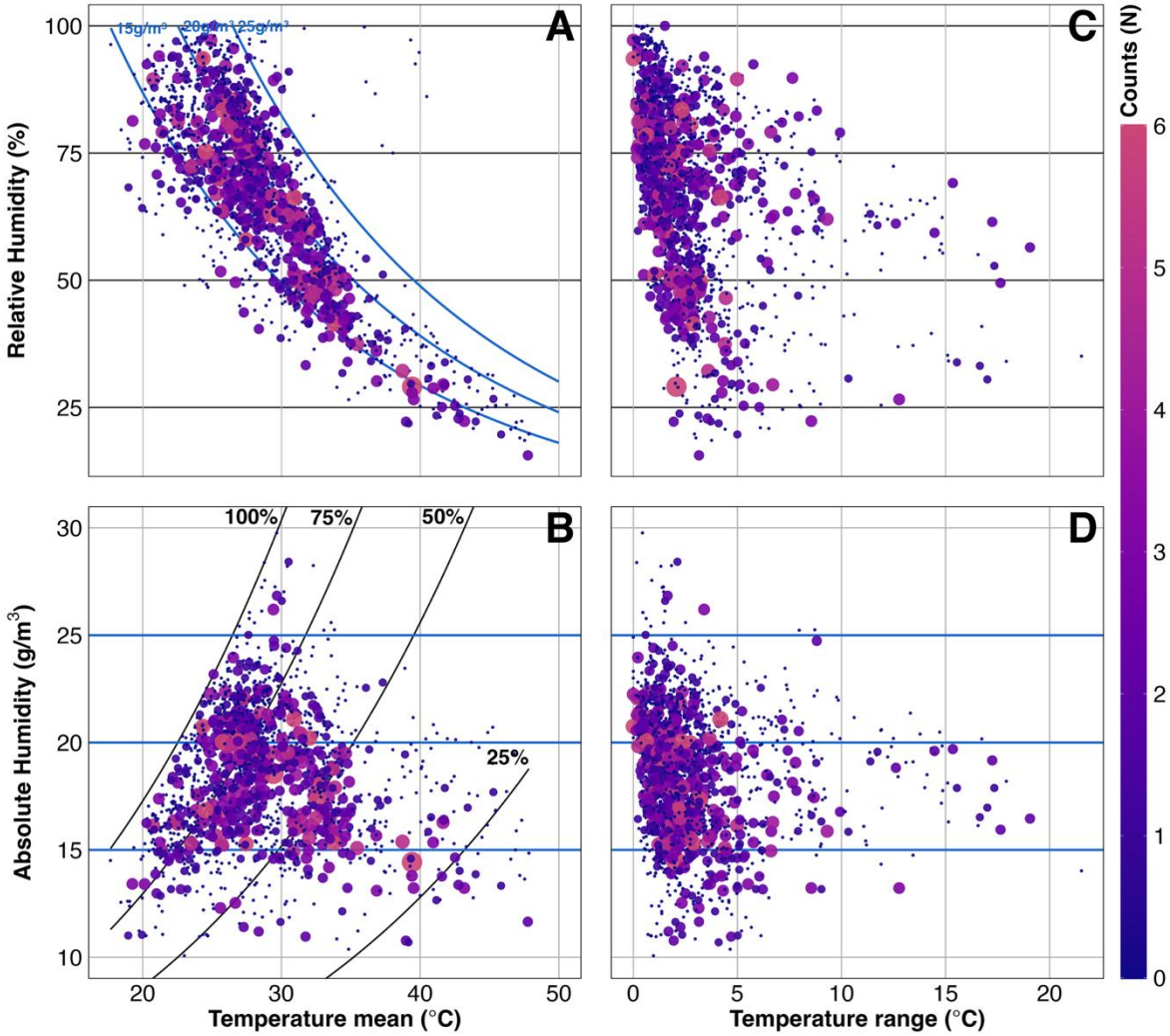


Figure 5. Indoor microclimate and *Anopheles funestus* abundance. Datapoints show individual sampling results, where colour and size depict number of collected mosquitoes. (A-B) *An. funestus* abundance as a function of (A) mean temperature and relative humidity, and (B) mean temperature and absolute humidity. The black and blue curved and horizontal lines depict isolines of constant relative and absolute humidity, respectively (curved AH

isolines in A correspond to horizontal isolines in B and D; curved RH isolines in B correspond to horizontal isolines in A and C). Temperature and relative humidity are strongly negatively correlated (r = - 0.738), which reduces the statistical power to separate their respective effects on abundance. In contrast, temperature and absolute humidity show only weak correlation (r = 0.072), improving the ability to distinguish independent effects of temperature and humidity on abundance.

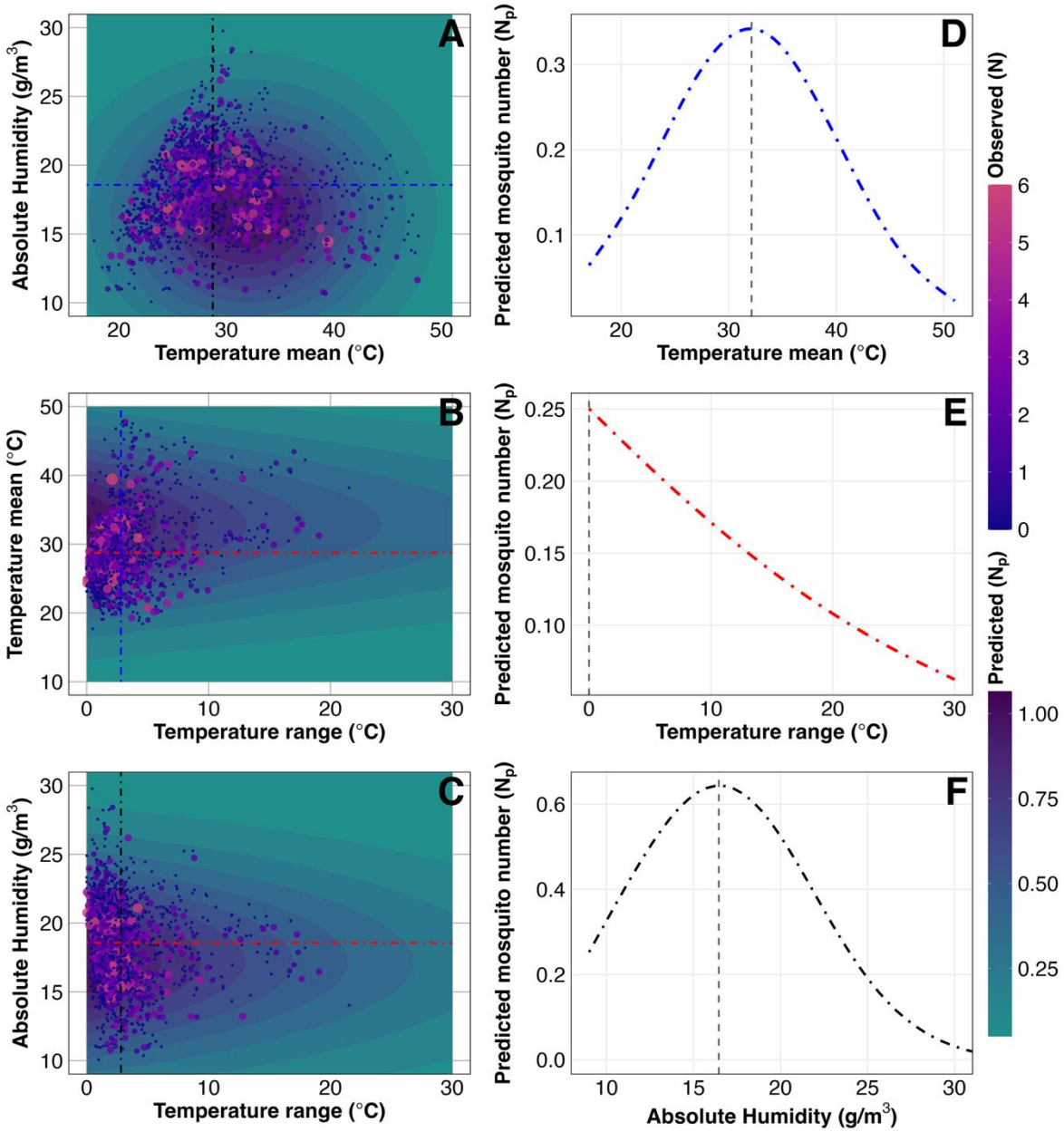
Table 2. Adjusted incidence rate ratios (aIRR) for *An. funestus* abundance across predictor categories, adjusted for indoor mean temperature and fluctuations (range), and mean absolute humidity and fluctuation (adjusted variance inflation factors (VIF ≤ 2)). Results are presented as the mean and 95% confidence intervals (95% CI) of the model-predicted aIRR per category, and the corresponding p-value. Significant p-values < 0.05 are highlighted in bold.

Predictors	**Categories**	**aIRR**		***p*-value**
		mean	**95% CI**	
Temperature	Mean ($\bar{T}$)	1.59	1.41 - 1.80	**<0.001**
	Mean^2 ($\bar{T}^2$)	0.99	0.99 - 0.99	**<0.001**
	Range (T_{range})	0.94	0.92 - 0.97	**<0.001**
Absolute humidity	Mean ($\overline{AH}$)	1.77	1.42 - 2.22	**<0.001**
	Mean^2 ($\overline{AH}^2$)	0.98	0.98 - 0.99	**<0.001**
	Range (AH_{range})	1.03	0.99 - 1.08	0.140

Overall, *An. funestus* abundance was significantly associated with both mean temperature and absolute humidity, with evidence of non-linear relationships for both variables (**Table 2; Fig. 6**). Mean temperature was positively associated with mosquito abundance (aIRR = 1.59 [1.41 - 1.80], p < 0.001), while the negative quadratic term (aIRR = 0.99 [0.99 - 0.99], p < 0.001) indicated a unimodal response. Similarly, mean absolute humidity showed a positive association with mosquito abundance (aIRR = 1.77 [1.42 - 2.22], p < 0.001), whereas the significant negative quadratic term (aIRR = 0.98 [0.98 - 0.99], p < 0.001) suggested an optimum moisture level beyond which mosquito abundance declined. Temperature variability was negatively associated with mosquito abundance, with each unit increase in temperature range reducing expected mosquito counts by approximately 6% (aIRR = 0.94 [0.92 - 0.97], p < 0.001). In contrast, absolute humidity variability was not significantly associated with mosquito abundance (aIRR = 1.03 [0.99 - 1.08], p = 0.140).

The response surface showed that *An. funestus* abundance peaked under moderate temperature and humidity conditions (**Fig. 6A**), closely corresponding to the climatic conditions where the highest observed mosquito counts occurred. Marginal effect plots showed that mosquito abundance increased with mean temperature up to an optimum of approximately 32.7°C before declining sharply at higher temperatures (**Fig. 6D**). Similarly, abundance increased with mean absolute humidity up to approximately 16.4 g/m³ and subsequently decreased at higher moisture levels (**Fig. 6F**). Declined abundance at both lower and higher values of temperature and absolute humidity, confirmed the unimodal relationships identified by the significant quadratic terms in the regression model (**Table 2**).

Temperature variability exhibited a consistently negative effect on mosquito abundance where predicted numbers decreased progressively as temperature range increased (**Fig. 6E**). Mosquitoes were more abundant under thermally stable conditions, at temperature fluctuations approximately below 5°C. This pattern was evident in both the mean temperature against temperature range (**Fig. 6B**) and absolute humidity against temperature range (**Fig. 6C**) response surfaces. The clustering of observed mosquito catches within areas of low temperature variability supported this relationship.



463

464 **Figure 6.** Empirical and modelled effect of indoor microclimatic conditions on the in-house
465 resting abundance of *An. funestus*. (A-C) Combined effect of temperature (mean and range)
466 and absolute humidity on indoor mosquito resting abundance. Datapoints show individual
467 sampling results, where colour and symbol size depict number of collected mosquitoes (see
468 legend in A). The coloured contour plots show modelled resting abundance as a function of
469 microclimatic conditions, based on the sampled data (see the legend in C). The different
470 panels show *An. funestus* abundance as a function of (A) mean temperature and absolute
471 humidity, (B) mean temperature and temperature range, and (C) temperature range and
472 absolute humidity. (D-F) The isolated effects of (D) mean temperature, (E) temperature
473 range, and (F) absolute humidity on *An. funestus* resting abundance, as estimated by the

generalized linear model with quadratic function. The coloured dot-dashed curves show predicted mosquito abundance as a function of the specific microclimate parameter, while keeping the other parameters constant at the mean value. The specific curves in (D-F) correspond to the same-coloured dot-dashed lines in (A-C). These combined results show that mosquito abundance peaks at a mean temperature of approximately 32.7ºC (A, B, D), an absolute humidity of 16.4 g/m^3 (A, C, F), and when temperature fluctuations are minimal (B, C, E).

Molecular analysis and fitness parameters

A total of 384 blood-fed *An. funestus* group specimens were analysed to determine sibling species composition, blood meal sources, and *P. falciparum* infection status. PCR amplification success was 98% (n = 375). Of these, 98% (n = 367) were identified as *An. funestus s.s*, while a small proportion were identified as *An. rivulorum* (1.6%, n = 6) and *An. leesoni* (n = 2). Among the 367 *An. funestus* s.s individuals, six individuals (1.6%) were positive for *P. falciparum* sporozoites and exclusively detected to have fed on human blood. Of the 384 engorged mosquitoes analysed for blood meal origin, 92% (n = 352) had fed exclusively on humans. Of the remaining 8%, 12 comprised of mixed blood meals including human-goat (n = 1), human-bovine (n = 1), human-chicken (n = 8), and human-dog (n = 2), whereas 20 yielded no identifiable blood source.

Species-specific analysis showed that 94% (n = 344) of *An. funestus* s.s. had exclusively fed on humans, 3% (n = 11) yielded no detectable blood meal source, and the remainder had mixed blood meals, including human-chicken (n = 8), human-dog (n = 2), human-bovine (n = 1), and human-goat (n = 1). Among *An. rivulorum* (n = 6), 50% (n = 3) had fed on humans, while the remaining three specimens had no detectable blood meal source. Of the 26 mosquitoes that were not successfully identified to sibling species, 65% (n = 17) had non-detectable blood meal source, 27% (n = 7) had fed on humans, and 8% (n = 2) had mixed human-dog blood meals.

Discussion

Malaria vector control strongly relies on understanding how mosquitoes interact with their environment during larval development, blood-feeding, and resting periods. The post-feeding resting phase provides a critical opportunity for vector control interventions [51–53]. However, resting behavioural shifts away from wall surfaces towards alternative sites,

including under-roof spaces, lower wall sections, floors, and household items, may alter the effectiveness of conventional strategies [10]. In the present study, *An. funestus* predominantly rested on the lower sections of house walls and floors, whereas only approximately one-third of mosquitoes occupied mid-wall surfaces traditionally targeted by control interventions. These findings are consistent with reports from other sub-Saharan African settings demonstrating that a substantial proportion of *An. funestus* rest on non-wall surfaces [10,13,14,19,20]. Collectively, these observations support the need for understanding species-specific resting behaviours and fine-scale environmental heterogeneity within houses [13,15–17].

Simultaneous evaluation of indoor mosquito resting distribution and diurnal microclimatic conditions revealed a vertical temperature and humidity stratification within houses. Lower house sections consistently represented the coolest indoor microhabitats, whereas upper sections were the warmest, particularly during warmer months (**Fig. 3**). Consistent with Okech *et al*. [11,12], temperature and humidity-driven microhabitats exist even within individual houses. Observed resting distributions are likely to reflect ecological responses to indoor microclimatic conditions rather than insecticide-induced behavioural avoidance since IRS has never been implemented in the study area [54]. Housing construction materials substantially modified these microclimatic gradients. Grass-thatched and mud-walled houses maintained cooler and less variable indoor conditions than metal-roofed and brick-walled houses, while upper house sections and metal-roofed houses experienced the greatest temperature fluctuation (**Fig. 3 & 4**). Humidity patterns showed similar heterogeneity, with house materials, indoor zones, and periods of the day that were associated with higher temperature consistently exhibiting lower humidity levels than their counterparts (**Fig. 3**). Sampling time, roof material, and indoor zone exerted both statistically significant and biologically meaningful effects on humidity, whereas wall material showed a weaker, although significant, influence. Together, these findings demonstrate substantial heterogeneity in indoor thermal and moisture conditions, with warmer environments tending to be consistently drier. Therefore, traditional houses which are being replaced or modified with metal-sheet roofs, brick or cement walls with altered ventilation systems might substantially alter mosquito resting dynamics [21–23]. For instance, metal-sheet roofs often enhance daytime heat accumulation, and drier air might discourage indoor resting unlike grass-thatched roofs which provide more thermally buffered and stable conditions [24].

Although these observations suggest a strong influence of indoor microclimate on mosquito resting behaviour, identifying the specific environmental drivers require a more detailed examination of temperature and moisture effects. In this study, temperature and relative humidity were strongly negatively correlated, limiting the ability to disentangle their independent effects on mosquito abundance. In contrast, temperature and absolute humidity (AH) exhibited only a weak correlation, allowing clearer separation of the influences of temperature and atmospheric moisture or resting behaviour. Therefore, absolute humidity rather than relative humidity is the better environmental variable to predict mosquito thermal biology since it quantifies the actual water content in air independent of temperature [55]. Two-dimensional response surface analysis indicated that mosquito abundance peaked within moderate temperature (25 - 35 °C) and AH (15 - 25 g/m³) ranges, declining sharply under hotter or drier conditions (**Fig. 6**). Importantly, microclimatic variability appeared to be more influential than mean temperature alone. Increased temperature fluctuations were associated with reduced mosquito densities, highlighting the importance of thermal stability in shaping *An. funestus* resting site selection (**Table 2; Fig. 6**).

Collectively, these findings indicate that indoor *An. funestus* abundance is maximized under thermally stable, moderately warm conditions with sustained atmospheric moisture. Consistent with previous studies, this suggests a negative effect of thermal variability on larval development rates and adult survival of malaria vectors [56,57]. The observed preference for cooler and more thermally stable resting locations suggests that lower house surfaces may function as microrefugia, particularly during periods of elevated environmental temperatures. Such microhabitats may buffer mosquitoes against thermal stress and desiccation, thereby sustaining vector populations, whereas elevated temperatures combined with low humidity are likely to accelerate water loss and reduce survival [58]. More broadly, these findings highlight the interactive effects of temperature and atmospheric moisture on mosquito ecology and vectorial capacity [30,55], supporting the hypothesis that *An. funestus* selectively occupies microhabitats that optimise physiological performance while minimizing desiccation risk. Furthermore, declined abundance at both lower and higher values of temperature and absolute humidity suggest that *An. funestus* occupies a restricted microclimatic niche. This pattern agrees with thermal performance theory, where ectotherm performance peaks within an optimal environmental range and declines beyond physiological limits [26,55].

While the study provides evidence linking indoor microclimatic conditions to resting behaviour, several limitations should be considered when interpreting these findings. First, houses were purposefully selected to represent common construction materials, which may limit the generalisability of results beyond the study area. Second, the observational design precludes definitive inference regarding causal relationships between microclimatic conditions and mosquito resting preferences. Additional household-level factors, including house size, eave openness, occupancy, bed-net use, indoor clutter, livestock proximity, and distance to larval habitats, may also have influenced mosquito abundance and resting behaviour. Finally, although temperature and humidity were measured at high spatial and temporal resolution, the study did not directly assess mosquito survival, movement, exit behaviour, or malaria transmission outcomes. Future experimental studies and housing-modification trials are needed to determine whether manipulating indoor microclimates can reduce resting suitability and improve vector control effectiveness.

Conclusion

This study demonstrates that the indoor resting behaviour of *An. funestus* is strongly shaped by fine-scale microclimatic conditions generated by house structure and environmental variation. Mosquitoes preferentially occupied cooler and more thermally stable microhabitats, particularly in the lower section of houses, while abundance declined under hotter and drier conditions. Future investigations of malaria vector ecology should prioritize absolute humidity rather than relative humidity when assessing microclimatic effects, as it provides a more independent measure of atmospheric moisture and allows clearer interpretation. Together, these findings highlight the importance of incorporating indoor microclimatic heterogeneity into vector surveillance and control strategies. Therefore, housing improvements could reduce indoor environmental suitability for mosquito resting and thus reduced malaria transmission risk.

List of symbols

N; Number of sampled resting mosquitoes, *n;* Relative number of sampled resting mosquitoes, P; Proportion of resting mosquitoes, ($\hat{\mu}$); Estimated relative number of resting mosquitoes, *T;* Temperature, $\bar{T}$; Mean temperature, T_{range}; Temperature range, RH; Relative humidity, $\overline{RH}$; Mean relative humidity, RH_{range}; Relative humidity range, AH; Absolute humidity, $\overline{AH}$; Mean absolute humidity, AH_{range}; Absolute humidity range, Δ; Difference, d; Cohen's d, p; p-value.

Abbreviations

COVID-19; SARS corona virus disease 2019, WHO; World Health Organization, ITS2; Internal Transcribed Spacer 2, DNA; Deoxyribonucleic Acid, IRS; Indoor Residual Spraying, GLM; Generalized Linear Model, GAM; Generalized Additive Model, aIRR; Adjusted Incidence Rate Ratios, AIC; Akaike Information Criterion, BIC; Bayesian Information Criterion, H; Humidity, AH; Absolute Humidity, RH; Relative Humidity

Ethics approval and consent to participate

This study was permitted by the Institute Review Board of Ifakara Health Institute; IHI/IRB/EXT/No: 24-2023 and the Medical Research Coordinated Committee of the National Institute for Medical Research of the United Republic of Tanzania; NIMR/HQ/R.8c/Vol.I/2985.

Consent for publication

This manuscript has been approved for publication by the National Institute for Medical Research of the United Republic of Tanzania (Ref No. BD.242/437/01D/198).

Availability of data and materials

Data are available under the Ifakara Health Institute and Wageningen University & Research data sharing policy upon request and approval.

Competing interests

The authors declare that they have no competing interests.

Funding

The activities in this work were funded by the Wellcome Trust- Infectious Disease-Discretionary grant (Grant Number: 226703/Z/22/Z) and Gates Foundation (Grant Number: NV-043574) awarded to Emmanuel W. Kaindoa.

Author contributions

PGP, EWK, FOO, FTM, AC and CJMK conceptualized the idea, designed the study, supervised the experiments and drafted the manuscript; PGP analysed the data and drafted the manuscript; DEN, MRR, IH conceptualized the idea, mobilized funding and manuscript drafting; DSM, GM, and SM helped to design the study, supervised the experiments; GM and

SM helped with the field mosquito collection and morphological identification. All authors read and approved the final manuscript.

Acknowledgements

We thank the Ifakara Health Institute research team for their great support and community members who volunteered their houses for mosquito collections.

References

1. WHO. World malaria report 2024 Addressing inequity in the global malaria response [Internet]. Geneva; 2024 Dec. Available from: https://www.who.int/teams/global-malaria-programme/reports/world-malaria-report-2024

2. WHO. World malaria report 2025: addressing the threat of antimalarial drug resistance [Internet]. Geneva; 2025. Available from: https://www.who.int/publications/i/item/9789240117822

3. WHO. World malaria report 2023 Tracking progress and gaps in the global response to malaria [Internet]. Geneva; 2023 Nov. Available from: https://www.who.int/teams/global-malaria-programme/reports/world-malaria-report-2023

4. Bhatt S, Weiss DJ, Cameron E, Bisanzio D, Mappin B, Dalrymple U, et al. The effect of malaria control on *Plasmodium falciparum* in Africa between 2000 and 2015. Nature. 2015;526:207–11.

5. Raghavendra K, Barik TK, Reddy BPNN, Sharma P, Dash AP. Malaria vector control: From past to future. Parasitol Res. 2011;108:757–779.

6. Okumu F. The fabric of life: what if mosquito nets were durable and widely available but insecticide-free? Malar J 2020 191. 2020;19:260.

7. Protopopoff N, Mosha JF, Lukole E, Charlwood JD, Wright A, Mwalimu CD, et al. Effectiveness of a long-lasting piperonyl butoxide-treated insecticidal net and indoor residual spray interventions, separately and together, against malaria transmitted by pyrethroid-resistant mosquitoes: a cluster, randomised controlled, two-by-two fact. Lancet. 2018;391:1577–88.

8. Yukich J, Digre P, Scates S, Boydens L, Obi E, Moran N, et al. Incremental cost and cost-

effectiveness of the addition of indoor residual spraying with pirimiphos-methyl in sub-Saharan Africa versus standard malaria control: results of data collection and analysis in the Next Generation Indoor Residual Sprays (NgenIR. Malar. J. 2022. p. 185.

9. Oxborough RM. Trends in US President's Malaria Initiative-funded indoor residual spray coverage and insecticide choice in sub-Saharan Africa (2008-2015): urgent need for affordable, long-lasting insecticides. Malar J. 2016;15:146.

10. Irish SR, Nimmo D, Bharmel J, Tripet F, Müller P, Manrique-Saide P, et al. A review of selective indoor residual spraying for malaria control. Malar J. 2024;23:252.

11. Okech BA, Gouagna LC, Killeen GF, Knols BGJ, Kabiru EW, Beier JC, et al. Influence of Sugar Availability and Indoor Microclimate on Survival of *Anopheles gambiae* (Diptera: *Culicidae*) Under Semifield Conditions in Western Kenya. J Med Entomol. 2003;40:657–63.

12. Okech BA, Gouagna LC, Knols BGJ, Kabiru EW, Killeen GF, Beier JC, et al. Influence of indoor microclimate and diet on survival of *Anopheles gambiae* ss (Diptera: *Culicidae*) in village house conditions in western Kenya. Int J Trop Insect Sci. 2004;24:207–12.

13. Chabi J, Seyoum A, Edi CVA, Kouassi BL, Yihdego Y, Oxborough R, et al. Efficacy of partial spraying of SumiShield, Fludora Fusion and Actellic against wild populations of *Anopheles gambiae* s.l. in experimental huts in Tiassalé, Côte d'Ivoire. nature.com. 2023;13:11364.

14. Coleman S, Yihdego Y, Sherrard-Smith E, Thomas CS, Dengela D, Oxborough RM, et al. Partial indoor residual spraying with pirimiphos-methyl as an effective and cost-saving measure for the control of *Anopheles gambiae* sl in northern Ghana. nature.com. 2021;11:18055.

15. Arredondo-Jimenez JI, Bown DN, Rodriguez MH, Loyola EG. Control of *Anopheles albimanus* mosquitos in southern Mexico by spraying their preferred indoor resting sites. Bull World Health Organ. 1995;73:329–37.

16. Asinas CY, Hugo CT, Boase CJ, Evans RG. Evaluation of selective spraying of bendiocarb (Ficam VC) for the control of *Anopheles flavirostris* in the Philippines. J Am Mosq Control Assoc. 1994;10:496–500.

685 17. Gandahusada S, Fleming GA, Sukamto, Damar T, Suwarto, Sustriayu N, et al. Malaria
686 control with residual fenitrothion in Central Java, Indonesia: an operational-scale trial using
687 both full and selective coverage treatments. Bull World Health Organ. 1984;62:783.

688 18. Osae M. Resting behaviour of endophilic *Anopheline* vectors in three ecological zones of
689 southern Ghana and its implications for the use of entomopathogenic fungi [Internet].
690 Doctoral dissertation, University of Ghana; 2014 [cited 2025 Nov 11]. Available from:
691 https://ugspace.ug.edu.gh/items/511faf61-c106-4491-84ef-caa7534d5212

692 19. Sande S, Zimba M, Chinwada P, Masendu HT, Makuwaza A. Insights into Resting
693 Behavior of Malaria Vector Mosquitoes in Mutare and Mutasa Districts of Manicaland
694 Province, Zimbabwe. J Med Entomol. 2016;53:866–72.

695 20. Msugupakulya BJ, Kaindoa EW, Ngowo HS, Kihonda JM, Kahamba NF, Msaky DS, et
696 al. Preferred resting surfaces of dominant malaria vectors inside different house types in rural
697 south-eastern Tanzania. Malar J. 2020;19:22.

698 21. Tusting LS, Bisanzio D, Alabaster G, Cameron E, Cibulskis R, Davies M, et al. Mapping
699 changes in housing in sub-Saharan Africa from 2000 to 2015. Nature. 2019;568:391–4.

700 22. Tusting LS, Ippolito MM, Willey BA, Kleinschmidt I, Dorsey G, Gosling RD, et al. The
701 evidence for improving housing to reduce malaria: a systematic review and meta-analysis.
702 Malar J 2015 141. 2015;14:209.

703 23. Lindsay SW, Emerson PM, Charlwood JD. Reducing malaria by mosquito-proofing
704 houses. Trends Parasitol. 2002;18:510–4.

705 24. Musiime AK, Krezanoski PJ, Smith DL, Kilama M, Conrad MD, Otto G, et al. House
706 design and risk of malaria, acute respiratory infection and gastrointestinal illness in Uganda: a
707 cohort study. journals.plos.org. 2022;2:e0000063.

708 25. Thomas MB, Blanford S. Thermal biology in insect-parasite interactions. Trends Ecol
709 Evol. 2003;18:344–50.

710 26. Mordecai EA, Caldwell JM, Grossman MK, Lippi CA, Johnson LR, Neira M, et al.
711 Thermal biology of mosquito-borne disease. Ecol Lett. 2019;22:1690–708.

712 27. Christiansen-Jucht C, Parham PE, Saddler A, Koella JC, Basáñez M-G. Temperature

during larval development and adult maintenance influences the survival of *Anopheles gambiae s.s.* Parasit Vectors. 2014;7:489.

28. Aytekin S, Aytekin AM, Alten B. Effect of different larval rearing temperatures on the productivity (Ro) and morphology of the malaria vector *Anopheles superpictus Grassi* (Diptera: *Culicidae*) using geometric morphometrics. J Vector Ecol. 2009;34:32–42.

29. Barreaux AMG, Stone CM, Barreaux P, Koella JC. The relationship between size and longevity of the malaria vector *Anopheles gambiae (s.s.)* depends on the larval environment. Parasit Vectors. 2018;11:485.

30. Danlami G, Isah B, Odeyemi M, Ukubuiwe A. Indoor behaviour responses of the principal malaria vector, *Anopheles gambiae* (Diptera: *Culicidae*), in relation to micro-climatic conditions in Minna, North. Res J Parasitol. 2011;6:109–15.

31. Agyekum TP, Botwe PK, Arko-Mensah J, Issah I, Acquah AA, Hogarh JN, et al. A systematic review of the effects of temperature on mosquito development and survival: Implications for malaria control in a future warmer climate. Int J Environ Res Public Health. 2021;18:7255.

32. Ngowo HS, Kaindoa EW, Matthiopoulos J, Ferguson HM, Okumu FO. Variations in household microclimate affect outdoor-biting behaviour of malaria vectors. Wellcome open Res. 2017;2:102.

33. Dery DB, Brown C, Asante KP, Adams M, Dosoo D, Amenga-Etego S, et al. Patterns and seasonality of malaria transmission in the forest-savannah transitional zones of Ghana. Malar J. 2010;9:314.

34. Kelly-Hope LA, Hemingway J, McKenzie FE. Environmental factors associated with the malaria vectors *Anopheles gambiae* and *Anopheles funestus* M in Kenya. Malar J. 2009;8:268.

35. Asigau S, Parker PG. The influence of ecological factors on mosquito abundance and occurrence in Galápagos. J Vector Ecol. 2018;43:125–37.

36. Barbosa LMC, Souto RNP, Ferreira RM dos A, Scarpassa VM. Composition, abundance and aspects of temporal variation in the distribution of *Anopheles* species in an area of

741 Eastern Amazonia. Rev Soc Bras Med Trop. 2014;47:313–20.

742 37. Spark Weather. Climate and Average Weather Year Round in Ifakara, Tazania [Internet].
743 [cited 2026 Apr 29]. Available from: https://weatherspark.com/y/99526/Average-Weather-in-
744 Ifakara-Tanzania-Year-Round

745 38. Kaindoa EW, Matowo NS, Ngowo HS, Mkandawile G, Mmbando A, Finda M, et al.
746 Interventions that effectively target *Anopheles funestus* mosquitoes could significantly
747 improve control of persistent malaria transmission in south–eastern Tanzania. PLoS One.
748 2017;12:e0177807.

749 39. Mapua SA, Hape EE, Kihonda J, Bwanary H, Kifungo K, Kilalangongono M, et al.
750 Persistently high proportions of *Plasmodium*-infected Anopheles funestus mosquitoes in two
751 villages in the Kilombero valley, South-Eastern Tanzania. Parasite Epidemiol Control.
752 2022;18:e00264.

753 40. Pinda PG, Eichenberger C, Ngowo HS, Msaky DS, Abbasi S, Kihonda J, et al.
754 Comparative assessment of insecticide resistance phenotypes in two major malaria vectors,
755 *Anopheles funestus* and *Anopheles arabiensis* in south-eastern Tanzania. Malar J.
756 2020;19:408.

757 41. Pinda PG, Msaky DS, Muyaga LL, Mshani IH, Njalambaha RM, Kihonda J, et al.
758 Relationships between biological age, distance from aquatic habitats and pyrethroid
759 resistance status of *Anopheles funestus* mosquitoes in south-eastern Tanzania. Malar J.
760 2022;21:365.

761 42. Vazquez-Prokopec GM, Galvin WA, Kelly R, Kitron U. A New, Cost-Effective, Battery-
762 Powered Aspirator for Adult Mosquito Collections. J Med Entomol. 2009;46:1256–9.

763 43. Coetzee M. Key to the females of Afrotropical *Anopheles* mosquitoes (Diptera:
764 *Culicidae*). Malar J. 2020;19:70.

765 44. Gillies MT, Coetzee M. A Supplement to the Anophelinae of the South of the Sahara
766 (Afrotropical Region). Publ South African Inst Med Res. 1987;55:1–143.

767 45. Koekemoer LL, Kamau L, Hunt RH, Coetzee M. A cocktail polymerase chain reaction
768 assay to identify members of the *Anopheles funestus* (Diptera : *Culicidae*) group. Am J Trop

769 Med Hyg. 2002;66:804–11.

770 46. Wirtz RA, Sattabongkot J, Hall T, Burkot TR, Rosenberg R. Development and Evaluation
771 of an Enzyme-Linked Immunosorbent Assay for *Plasmodium vivax*-VK247 Sporozoites. J
772 Med Entomol. 1992;29:854–7.

773 47. Durnez L, Van Bortel W, Denis L, Roelants P, Veracx A, Trung HD, et al. False positive
774 circumsporozoite protein ELISA: a challenge for the estimation of the entomological
775 inoculation rate of malaria and for vector incrimination. Malar J. 2011;10:195.

776 48. Chow E, Wirtz R, Scott T. Identification of blood meals in *Aedes aegypti* by antibody
777 sandwich enzyme-linked immunosorbent assay. Am Mosq Control Assoc. 1993;9:196–196.

778 49. R Core Team. R: A Language and Environment for Statistical Computing [Internet].
779 Vienna, Austria: R Foundation for Statistical Computing; 2025 [cited 2025 Nov 28].
780 Available from: https://www.r-project.org/

781 50. Russell V. Lenth. emmeans: Estimated Marginal Means, aka Least-Squares Means
782 [Internet]. 2025 [cited 2025 Nov 28]. Available from: https://cran.r-
783 project.org/package=emmeans

784 51. Jones, M. D.R. Gubbins SJ. Changes in the circadian flight activity of the mosquito
785 *Anopheles gambiae* in relation to insemination, feeding and oviposition. Physiol Entomol.
786 1978;3:213–20.

787 52. Takken W, Van Loon JJA, Adam W. Inhibition of host-seeking response and olfactory
788 responsiveness in *Anopheles gambiae* following blood feeding. J Insect Physiol.
789 2001;47:303–10.

790 53. WHO. An operational manual for indoor residual spraying (IRS) for malaria transmission
791 control and elimination. World Heal. Organ. Geneva; 2015.

792 54. Nagpal BN, Srivastava A, Dash AP. Resting behaviour of *Anopheles stephensi* type form
793 to assess its amenability to control malaria through indoor residual spray. J Vector Borne Dis.
794 2012;49:175–80.

795 55. Brown JJ, Pascual M, Wimberly MC, Johnson LR, Murdock CC. Humidity – The
796 overlooked variable in the thermal biology of mosquito-borne disease. Ecol Lett.

2023;26:1029–49.

56. Davies C, Coetzee M, Lyons CL. Effect of stable and fluctuating temperatures on the life history traits of *Anopheles arabiensis* and *An. quadriannulatus* under conditions of inter- and intra-specific competition. Parasit Vectors. 2016;9:342.

57. Lyons CL, Coetzee M, Chown SL. Stable and fluctuating temperature effects on the development rate and survival of two malaria vectors, *Anopheles arabiensis* and *Anopheles funestus*. Parasit Vectors. 2013;6:104.

58. Schmidt CA, Comeau G, Monaghan AJ, Williamson DJ, Ernst KC. Effects of desiccation stress on adult female longevity in *Aedes aegypti* and *Ae. albopictus* (Diptera: *Culicidae*): results of a systematic review and pooled survival analysis. Parasites Vectors 2018 111. 2018;11:267.

Supplementary materials

Supplementary table S1. Adjusted incidence rate ratios (aIRR) for *An. funestus* abundance across predictor categories, adjusted for indoor mean temperature and fluctuations (range), and mean relative humidity and fluctuation. Results are presented as the mean and 95% confidence intervals (95% CI) of the model-predicted aIRR per category, and the corresponding *p*-value. Significant *p*-values < 0.05 are highlighted in bold.

Predictors	**Categories**	**aIRR**		***p*-value**
		mean	**95% CI**	
Temperature	Mean ($\bar{T}$)	1.36	1.18 - 1.57	**<0.001**
	Mean^2 ($\bar{T}^2$)	0.99	0.99 - 1.00	**<0.001**
	Range (T_{range})	0.97	0.92 - 1.01	0.146
Relative humidity	Mean ($\overline{RH}$)	1.01	0.98 - 1.04	0.649
	Mean^2 ($\overline{RH}^2$)	1.00	1.00 - 1.00	0.148
	Range (RH_{range})	0.99	0.98 - 1.01	0.419